PHILOSOPHICAL TRANSACTIONS OF THE ROYAL SOCIETY A MATHEMATICAL, PHYSICAL & ENGINEERING SCIENCES

Finite Element Solution of Boundary-Value Problems with Non-Removable Singularities

L. S. D. Morley

Phil. Trans. R. Soc. Lond. A 1973 **275**, 463-488
doi: 10.1098/rsta.1973.0112

FINITE ELEMENT SOLUTION OF BOUNDARY-VALUE PROBLEMS WITH NON-REMOVABLE SINGULARITIES

By L. S. D. MORLEY
Structures Department, Royal Aircraft Establishment, Farnborough

(*Communicated by E. H. Mansfield, F.R.S.* – *Received* 8 *February* 1973 – *Revised* 22 *June* 1973)

CONTENTS

The engineer is frequently confronted with the need to solve boundary-value problems where the first derivative, for example, of the solution is discontinuous at one or more points. Solution of such problems by ordinary application of the finite element scheme often proves unsatisfactory when the 'singularity' is of the type which cannot be removed at the start of the calculation.

The paper illustrates some of the consequences which arise from these ordinary solutions and then demonstrates a process of solution which makes use of a modified Rayleigh–Ritz method. The modification provides a practical and versatile mode of calculation which allows extensive exploitation of the singular functions in augmenting the piecewise polynomials of the finite element scheme. Details of tests are given which help in assessing the accuracy of the numerical results.

An important engineering activity concerns the fracture mechanics study of cracked structures where prediction of safety is based upon the value of the stress intensity factor as calculated from a linear elastic analysis. The stress intensity factor is a measure of the amplitude of the dominant singularity at the ends of the crack and examples are given of its calculation using the modified Rayleigh–Ritz method.

1. Introduction

A Discussion Meeting was held in June 1970 at the Royal Society on the numerical solution of partial differential equations. A recurrent feature in the Discussion concerned the difficulties which are encountered in obtaining a satisfactory solution accuracy and rate of convergence (Walsh 1971; Fox 1971; Whiteman 1971) in boundary-value problems where there are

non-removable singularities such as occur at points of discontinuity. Emphasis was given to the underlying mathematics and in applications to the method of finite differences. The present purpose is to provide contrast by illustrating a finite element scheme which takes advantage of a recent modification to the Rayleigh–Ritz method (Morley 1969, 1970). The modification provides an essentially practical, but well founded, and very versatile mode of calculation. It separates the calculation into distinct stages and permits a more extensive exploitation of the available singular functions than that recently described by Fix (1969) who also augments the piecewise polynomials of the ordinary finite element scheme.

Finite elements may be regarded as a means of piecewise application of the Rayleigh–Ritz principle and, in view of the numerical complexities which are associated with the solution of even the simplest boundary-value problem, it is considered appropriate here to commence with numerical experiments on a one-dimensional interpolation problem. This sets out to provide a piecewise linear representation $u(x)$ of a given singular function $u^*(x)$ over $x_0 \leqslant x \leqslant x_N$ such that some functional $D(u^* - u)$ is minimized. Now, the term 'singular' is freely used whenever rather exceptional circumstances are encountered, but experience with this simple problem highlights the natural definition in the context of a piecewise method of solution. Theory predicts that a 'best' rate of convergence is available as the piecewise linear representation advances to successively finer uniform interval lengths $(x_N - x_0)/N$ when $u^*(x)$ has a continuous second derivative over $x_0 \leqslant x \leqslant x_N$ which has a maximum modulus M_2. The quantity $[D(u^* - u)]^{\frac{1}{2}}$ provides a convenient norm with which to measure the error and one hopes, in a practical situation, that this error diminishes at the 'best' convergence rate even starting with moderately large interval lengths. Our numerical experiments on the one-dimensional problem convince us that a marked deterioration in convergence rate occurs when M_2 does not exist. This leads to the essentially practical definition that $u^*(x)$ is singular in a piecewise linear representation whenever M_2 does not exist; there is a natural extension of the definition to higher degree representations. It also transpires that even the best convergence rate in a piecewise linear representation is too slow for most practical purposes and theory predicts now that solution accuracy is related to the actual magnitude of M_2. Thus, if we do not wish to further restrict the class of problems which might be considered amenable to practical solution by piecewise linear means, it is inevitable that attention be paid not only to the existence of M_2 but also to its magnitude. A mitigating feature is that the analytic structure, but not necessarily the amplitude, of these singularities and near singularities is predictable for many of the boundary-value problems which occur in practice. Clearly, when these analytic structures are incorporated into the solution process we seek to retain those agreeable characteristics, so important in engineering applications, which belong to the finite element technique – like positive definiteness, bandedness/sparseness of the assembled simultaneous equations for the nodal variables. All this can be achieved with the modified Rayleigh–Ritz principle and, in this one-dimensional problem, a quite exceptional accuracy is readily obtained for just one piecewise interval over the complete range $x_0 \leqslant x \leqslant x_N$. Furthermore, the numerical evidence from this example shows that solved quantities such as u may be effectively expressed in the form $u = u'(1 + cN^{-\gamma})$ over a wide range of values of the integer N which controls the interval/mesh size. Here, u', c, γ are constants where u' is the extrapolation of u for very large values of N, while if $|c| \ll 1$ then the solution is satisfactory for small N; the positive constant γ is a measure of the rate of convergence which is actually achieved. Much use is made of such formulae in assessing the merit of results obtained in the sequel.

After this preliminary, attention is duly given to numerical experiments on boundary-value

problems which have arisen out of practical situations. The first concerns a much studied plane harmonic mixed boundary-value problem with non-removable singularity; it was treated some time ago by Motz (1946), subsequently by Woods (1953) and more recently and notably by Whiteman (1971) at the Discussion Meeting, but a wholly satisfactory numerical solution is still awaited. The favoured solution process has, so far, been largely by the method of finite differences with, or without, special representation of the behaviour near the singular point. The boundary is of rectangular shape and here the whole enclosed region is partitioned by a uniform mesh of triangular finite elements; the piecewise Rayleigh–Ritz coordinate functions are then considered to vary linearly over each element with proper matching conditions along the edges. Theoretical work by Zlamal (1968) shows that the best rate of convergence as well as solution accuracy is again related to the existence and magnitude of M_2. Solutions of the homogeneous field equation are then given which describe the analytical structure at the singular point and it is noted that this problem has a nested double singularity in relation to a piecewise linear solution. These singular functions are then allowed to range over the whole enclosed region because this offers very definite practical advantages. For example, exactly satisfying the homogeneous field equation implies that this representation of the singular behaviour can be readily disassociated (by Green's formula) from the ingredient surface integrations of the finite element method. Three sets of results from finite element experiments are presented; the first does not recognize the presence of the singularity and the results for neighbouring points show considerable disparity from Whiteman's benchmark values. The second experiment incorporates terms which are capable not only of formally reproducing the analytic structure at the singular point, but also of satisfying exactly *all* the Rayleigh–Ritz subsidiary conditions on the boundary. Application of the modified Rayleigh–Ritz method then provides a somewhat improved set of results. In the third experiment, the simplest form of representation of the analytic structure is adopted with the Rayleigh–Ritz subsidiary conditions satisfied only in a piecewise linear sense. These are the most convincing results and are likely to be satisfactory for practical purposes. The conclusion to be drawn from these experiments is that the actual choice of terms to describe the singularity, or near singularity, is of special importance in achieving a successful numerical solution by practical means.

The paper concludes with application of the method to the plane stress elastic analysis of plates which contain a crack. This class of problem is of importance to engineers and occurs in fracture mechanics – which is the study of structural failure by catastrophic crack propagation at average stresses well below yield strength. In fracture mechanics, prediction of safety is based in the first instance upon the amplitude of the dominant stress singularity, i.e. the so-called stress intensity factor, as calculated from the elastic analysis of the cracked structure. The economic ramifications of these problems are clearly far reaching and so it is understandable that they have attracted considerable attention from engineers over the years with the result that there is now a substantial body of information available for the more standard configurations and loadings. Present-day efforts are largely directed towards establishing numerical methods which allow stress intensity factors to be calculated in a practical manner for the most complex structural configurations. The modified Rayleigh–Ritz method is well suited to these circumstances and, in contrast with many of its alternatives, is well founded and versatile. Moreover, it is foreseen that the method will have useful application in the relatively unexplored study of crack propagation in solids as well as in anisotropic materials.

Acknowledgement is made to the invaluable assistance of S. W. Nicolson, a sandwich student from the Department of Mathematics at the University of Surrey, throughout the computations.

PHILOSOPHICAL TRANSACTIONS OF THE ROYAL SOCIETY A MATHEMATICAL, PHYSICAL & ENGINEERING SCIENCES

2. One-dimensional interpolation problem

The purpose in beginning with a simple interpolation problem is to illustrate some of the difficulties and to accumulate experience helpful in the solution of real boundary-value problems with non-removable singularities.

The chosen one-dimensional interpolation problem concerns, initially, the piecewise linear continuous representation $u(x)$ of a given continuous function $u^*(x)$ so that

$$u^*(x) \simeq u(x) \quad (x_0 \leqslant x \leqslant x_N), \tag{2.1}$$

where there are N equally spaced intervals. Define the jth interval to lie between the coordinate positions $x = x_{j-1}$ and $x = x_j$ so that the linear representation in this interval may be written

$$u(x) = [N/(x_N - x_0)]\,[(x - x_{j-1})\,u(x_j) + (x_j - x)\,u(x_{j-1})] \quad (x_{j-1} \leqslant x \leqslant x_j). \tag{2.2}$$

The values of the $u(x_j)$ are to be determined so as to minimize a functional $D(u^* - u)$ which is defined as

$$D(u^* - u) = D(u^* - u, u^* - u) = \int_{x_0}^{x_N} \left(\frac{\mathrm{d}u^*}{\mathrm{d}x} - \frac{\mathrm{d}u}{\mathrm{d}x}\right)^2 \mathrm{d}x, \tag{2.3}$$

subject to the satisfaction of the subsidiary condition

$$u(x_0) = u^*(x_0). \tag{2.4}$$

Thus
$$\delta D(u^* - u) = -2D(u^* - u, \delta u) = 0 \tag{2.5}$$

for arbitrary variations $\delta u(x_j), j \to 1, 2, \ldots, N$, where

$$D(u^*, u) = \int_{x_0}^{x_N} \frac{\mathrm{d}u^*}{\mathrm{d}x}\frac{\mathrm{d}u}{\mathrm{d}x}\mathrm{d}x. \tag{2.6}$$

This minimization process provides a symmetric, banded, positive definite set of simultaneous equations to solve for the $u(x_j)$. Such equations are intrinsic to the finite element method and some very efficient solution procedures are available for use in conjunction with a digital computer. In the present instance, however, the banded equations are tridiagonal and the solution is given readily by

$$u(x_j) = u^*(x_j) \quad (j = 0, 1, 2, \ldots, N), \tag{2.7}$$

so that the piecewise linear representation interpolates $u^*(x)$ exactly at the nodal points x_j. In the subsequent computations it is useful to note that equations (2.4) and (2.5) provide

$$D(u^*, u) = D(u, u), \tag{2.8}$$

so that
$$D(u^* - u) = D(u^*) - D(u). \tag{2.9}$$

It is noted that all the above refers to an extraordinarily simple situation *vis-à-vis* the real boundary-value problem where u^* is never explicitly defined except possibly on the boundary.

To fix ideas, consider the piecewise linear representation of the continuous function

$$u^*(x) = (\sin x)^{\frac{3}{4}} \quad (0 \leqslant x \leqslant \tfrac{1}{2}\pi), \tag{2.10}$$

and introduce a quantity $E(u^* - u)$ which measures the averaged relative error of the piecewise representation by

$$E(u^* - u) = [D(u^* - u)/D_0]^{\frac{1}{2}}, \tag{2.11}$$

where D_0 is a constant defined by

$$D_0 = \int_0^{\frac{1}{2}\pi} \left\{ \frac{\mathrm{d}}{\mathrm{d}x} (\sin x)^{\frac{3}{4}} \right\}^2 \mathrm{d}x = 0.983271583. \tag{2.12}$$

Results of numerical experiments on the $u^*(x)$ of equation (2.10) are listed in table 1 where the relative error $E(u^* - u)$ is tabulated for a range of values of N. Experience with this kind of calculation shows that the behaviour of quantities like the relative error can be expressed quite accurately by

$$E(u^* - u) = cN^{-\gamma} \tag{2.13}$$

over a wide range of values of the integer N. In this equation, the magnitude of c when taken in comparison with unity provides a guide as to whether the solution is satisfactory for small (practical) values of N, while the positive constant γ measures the rate of convergence, i.e. the efficiency of the approximation procedure. Indeed, table 1 shows that near $N = 30$ the relative error behaves like

$$\left.\begin{aligned} E(u^* - u) &= 0.417N^{-0.26}, \\ &= 0.172 \quad \text{for} \quad N = 30. \end{aligned}\right\} \tag{2.14}$$

The large amplitude of this relative error at $N = 30$ shows that the ordinary piecewise linear representation of the $u^*(x)$ of equation (2.10) is not satisfactory and this conclusion is reinforced by the substantial value which is attained by c (0.417); with $\gamma = 0.26$ this solution is seen to be associated also with a very slow rate of convergence.

TABLE 1. RELATIVE ERRORS IN THE PIECEWISE LINEAR REPRESENTATION u OF THE GIVEN FUNCTION $u^* = (\sin x)^{\frac{3}{4}}$ OVER $0 \leqslant x \leqslant \frac{1}{2}\pi$

N	$E(u^* - u)$	$N^{0.26}E(u^* - u)$	N	$E(u^* - u)$	$N^{0.26}E(u^* - u)$
1	0.594	0.594	10	0.230	0.419
2	0.403	0.482	15	0.206	0.417
3	0.338	0.450	20	0.191	0.417
4	0.304	0.436	25	0.181	0.417
5	0.283	0.429	30	0.172	0.417

It is of interest to ascertain an upper bound on the relative error as well as to establish the best available rate of convergence in a more favourable context. This is readily achieved by noting that, because of equation (2.7),

$$\mathrm{d}u^*/\mathrm{d}x - \mathrm{d}u/\mathrm{d}x = 0 \quad \text{at some} \quad x = \xi \quad (x_{j-1} \leqslant \xi \leqslant x_j)$$

and hence

$$|\mathrm{d}u^*/\mathrm{d}x - \mathrm{d}u/\mathrm{d}x| \leqslant (x_N - x_0)\, M_2 N^{-1}, \tag{2.15}$$

where M_2 is the maximum modulus of the continuous second derivative of $u^*(x)$ over $x_0 \leqslant x \leqslant x_N$. When equation (2.15) is substituted into the functional of equation (2.3) integration provides

$$D(u^* - u) \leqslant (x_N - x_0)^3 M_2^2 N^{-2} \tag{2.16}$$

and so the relative error of equation (2.11) is bounded by

$$E(u^* - u) \leqslant [(x_N - x_0)^3 / D_0]^{\frac{1}{2}} M_2 N^{-1}. \tag{2.17}$$

This best rate of convergence $\gamma = 1$, see equation (2.13), is available for large enough N in a piecewise linear representation provided M_2 exists, while the accuracy, as measured by c, is related to

the actual magnitude of M_2. It therefore seems a natural consequence for us to refer, in the sequel, to $u^*(x)$ as being singular whenever M_2 does not exist.†

Now, the second derivative of the $u^*(x)$ of equation (2.10) is unbounded at $x = 0$ and so M_2 does not exist over the required interval $0 \leqslant x \leqslant \frac{1}{2}\pi$. The function is therefore singular and this is held to account for the unsatisfactory outcome from the above numerical experiments. A popular procedure to alleviate the ill effect in a boundary-value problem is to employ a special region near the singularity and then to continue with the ordinary numerical process elsewhere. This is used by Fox (1971) in the finite difference context while many authors commend their own super element in the finite element context. However, this involves some compromise because of the need to define, *ab initio*, the extent of the special region. Let us make a partial assessment of this kind of procedure by repeating the above experiments for the piecewise linear representation of

$$u^*(x) = (\sin x)^{\frac{3}{4}} \quad (0 < x_0 \leqslant x \leqslant \tfrac{1}{2}\pi), \tag{2.18}$$

TABLE 2. RELATIVE ERRORS IN THE PIECEWISE LINEAR REPRESENTATION u OF THE GIVEN FUNCTION $u^* = (\sin x)^{\frac{3}{4}}$ OVER $x_0 \leqslant x \leqslant \frac{1}{2}\pi$

	$x_0 = 0.01$		$x_0 = 0.02$		$x_0 = 0.05$		$x_0 = 0.20$	
N	$E(u^*-u)$	$N^{0.720}E(u^*-u)$	$E(u^*-u)$	$N^{0.825}E(u^*-u)$	$E(u^*-u)$	$N^{0.946}E(u^*-u)$	$E(u^*-u)$	$N^{0.998}E(u^*-u)$
1	0.524	0.524	0.500	0.500	0.458	0.458	0.355	0.355
2	0.317	0.523	0.293	0.520	0.255	0.491	0.183	0.366
3	0.244	0.539	0.219	0.543	0.183	0.516	0.124	0.371
4	0.205	0.556	0.180	0.564	0.144	0.536	0.094	0.373
5	0.179	0.570	0.154	0.582	0.120	0.550	0.075	0.376
10	0.118	0.619	0.095	0.635	0.067	0.589	0.038	0.379
15	0.091	0.642	0.070	0.656	0.047	0.603	0.025	0.379
20	0.075	0.652	0.056	0.665	0.036	0.607	0.019	0.380
25	0.064	0.655	0.047	0.666	0.029	0.608	0.015	0.380
30	0.056	0.654	0.040	0.665	0.024	0.607	0.013	0.380
M_2	59.3		25.0		8.0		1.6	

which avoids the singular point (cf. equation (2.10)). The numerical results are listed in table 2 for values of $x_0 = 0.01, 0.02, 0.05, 0.20$ and while these show, near $N = 30$, a marked improvement in the rate of convergence to $\gamma = 0.72$ for the smallest value $x_0 = 0.01$ (cf. equation (2.13) where $\gamma = 0.26$), it is not until $x_0 = 0.20$ that the best available rate is actually approached. However, for this very simple problem it seems unreasonable to be satisfied with a solution where the relative error $E(u^*-u) = 0.013$ is questionably negligible and is, moreover, still associated with a substantial value for $c(0.380)$. Reference values of M_2 are also listed in table 2. Furthermore, it is to be pointed out that the above provides a particularly favourable assessment of the special region procedure to the extent that the exact relation

$$u(x) \equiv u^*(x) \quad (0 \leqslant x \leqslant x_0) \tag{2.19}$$

is enforced.

Consider now a different approach which avoids the use of special regions and note also that while the structural shape of the singularity is predeterminable in simple terms for many boundary-value problems, the evidence suggests that this needs to be further supplemented to

† In extending this definition of singular $u^*(x)$ we note that it is directly dependent upon the polynomial degree of the piecewise representation. For example, the relative error $E(u^*-u)$ of a piecewise cubic representation may be shown to be proportional to $M_4 N^{-3}$ where M_4 is the maximum modulus of the fourth derivative of $u^*(x)$ over $x_0 \leqslant x \leqslant x_N$; in this case it would be appropriate to refer to $u^*(x)$ as being singular whenever M_4 does not exist.

achieve a satisfactory solution. Thus, the specific $u^*(x)$ which is defined by equation (2.10) may be expanded about the point at $x = 0$ in the form, say,

$$u^*(x) = (\sin x)^{\frac{3}{4}} = u_1^*(x) - \tfrac{1}{8}u_2^*(x) + \tfrac{7}{1920}u_3^*(x) - \ldots, \tag{2.20}$$

where

$$u_1^*(x) = x^{\frac{3}{4}}, \quad u_2^*(x) = x^{\frac{11}{4}}, \quad u_3^*(x) = x^{\frac{19}{4}}, \ldots. \tag{2.21}$$

The structure of the singularity itself is adequately described by just the first term $u_1^*(x)$ so that the remaining terms are characterized as supplementary. In boundary-value problems, however, it is only the structural shape of the individual terms in this expansion which is predeterminable so, typically, the only information known near the singular point is that

$$u^*(x) = \alpha_1 u_1^*(x) + \alpha_2 u_2^*(x) + \alpha_3 u_3^*(x) + \ldots, \tag{2.22}$$

where $u_1^*(x), u_2^*(x), u_3^*(x)$ are as given by equations (2.21) but the amplitudes $\alpha_1, \alpha_2, \alpha_3, \ldots$ are not known in advance. In seeking the most practical way of incorporating an equation like (2.22) into the piecewise linear approximation scheme, as typified by equations (2.1) to (2.9), we regard it to be particularly important neither to disturb the symmetric, banded, positive definite set of simultaneous equations from which the $u(x_j)$ are determined nor to modify the interval spacing. Accordingly, let us seek an approximate representation to the $u^*(x)$ of equation (2.10) through

$$u^* = (\sin x)^{\frac{3}{4}} \simeq u + \alpha_1(u_1^* - u_1) + \alpha_2(u_2^* - u_2) + \alpha_3(u_3^* - u_3) \quad (0 \leqslant x \leqslant \tfrac{1}{2}\pi), \tag{2.23}$$

where $u_1^*(x), u_2^*(x), u_3^*(x)$ are the function already defined by equations (2.21) and where, as yet, $u(x), u_1(x), u_2(x), u_3(x)$ are arbitrary continuous piecewise linear functions each taken over the same interval spacing with $\alpha_1, \alpha_2, \alpha_3$ as arbitrary constants. Next, minimize the functional, see equation (2.3),

$$D[u^* - u - \alpha_1(u_1^* - u_1) - \alpha_2(u_2^* - u_2) - \alpha_3(u_3^* - u_3)], \tag{2.24}$$

subject to the satisfaction of subsidiary conditions, see equation (2.4)

$$u(0) = u^*(0), \quad u_1(0) = u_1^*(0), \quad u_2(0) = u_2^*(0), \quad u_3(0) = u_3^*(0), \tag{2.25}$$

where the nodal values $u(x_j), u_1(x_j), u_2(x_j), u_3(x_j)$ of the piecewise linear functions, with $j = 1, 2, 3, \ldots, N$, as well as the constants $\alpha_1, \alpha_2, \alpha_3$ are to be subjected to arbitrary variation. This provides a minimization problem which requires satisfaction of the bilinear conditions.

$$\left.\begin{aligned}
&D[u^* - u - \alpha_1(u_1^* - u_1) - \alpha_2(u_2^* - u_2) - \alpha_3(u_3^* - u_3), \delta u] = 0,\\
&D[u^* - u - \alpha_1(u_1^* - u_1) - \alpha_2(u_2^* - u_2) - \alpha_3(u_3^* - u_3), \delta u_1] = 0,\\
&D[u^* - u - \alpha_1(u_1^* - u_1) - \alpha_2(u_2^* - u_2) - \alpha_3(u_3^* - u_3), \delta u_2] = 0,\\
&D[u^* - u - \alpha_1(u_1^* - u_1) - \alpha_2(u_2^* - u_2) - \alpha_3(u_3^* - u_3), \delta u_2] = 0,\\
&D[u^* - u - \alpha_1(u_1^* - u_1) - \alpha_2(u_2^* - u_2) - \alpha_3(u_3^* - u_3), (u_1^* - u_1)\,\delta\alpha_1] = 0,\\
&D[u^* - u - \alpha_1(u_1^* - u_1) - \alpha_2(u_2^* - u_2) - \alpha_3(u_3^* - u_3), (u_2^* - u_2)\,\delta\alpha_2] = 0,\\
&D[u^* - u - \alpha_1(u_1^* - u_1) - \alpha_2(u_2^* - u_2) - \alpha_3(u_3^* - u_3), (u_3^* - u_3)\,\delta\alpha_3] = 0.
\end{aligned}\right\} \tag{2.26}$$

Now, it is impossible to distinguish between the variations

$$\delta u(x_j), \quad \delta u_1(x_j), \quad \delta u_2(x_j), \quad \delta u_3(x_j) \tag{2.27}$$

and so the first four conditions of equations (2.26) are identical and are satisfied by making individually

$$\delta D(u^* - u) = \delta D(u_1^* - u_1) = \delta D(u_2^* - u_2) = \delta D(u_3^* - u_3) = 0, \tag{2.28}$$

subject, of course, to the satisfaction of the subsidiary conditions of equations (2.25). Thus u is identical with the ordinary piecewise linear representation developed through equations (2.1) to (2.9), while $u_1(x)$, $u_2(x)$, $u_3(x)$ are the ordinary piecewise linear representations respectively to $u_1^*(x)$, $u_2^*(x)$, $u_3^*(x)$. Moreover, and with reference to the general context, all these piecewise representations can be calculated simultaneously because of the complete identity in each instance between the associated band matrices. The last three conditions which are expressed by equations (2.26) allow the calculation of the constants α_1, α_2, α_3 from the three simultaneous linear equations

$$\begin{bmatrix} D(u_1^*-u_1) & D(u_1^*-u_1, u_2^*-u_2) & D(u_1^*-u_1, u_3^*-u_3) \\ & D(u_2^*-u_2) & D(u_2^*-u_2, u_3^*-u_3) \\ \text{sym.} & & D(u_3^*-u_3) \end{bmatrix} \begin{Bmatrix} \alpha_1 \\ \alpha_2 \\ \alpha_3 \end{Bmatrix} = \begin{Bmatrix} D(u_1^*-u_1, u^*-u) \\ D(u_2^*-u_2, u^*-u) \\ D(u_3^*-u_3, u^*-u) \end{Bmatrix}, \tag{2.29}$$

where we note that

$$\left.\begin{aligned} D(u_j^*-u_j, u_k^*-u_k) &= D(u_j^*, u_k^*) - D(u_j, u_k) \quad (j,k=1,2,3), \\ D(u_j^*-u_j, u^*-u) &= D(u_j^*, u^*) - D(u_j, u) \quad (j=1,2,3). \end{aligned}\right\} \tag{2.30}$$

TABLE 3. RELATIVE ERRORS ETC. IN THE APPROXIMATION
$u+\alpha_1(u_1^*-u_1)+\alpha_2(u_2^*-u_2)+\alpha_3(u_3^*-u_3)$
TO THE GIVEN FUNCTION $u^* = (\sin x)^{\frac{3}{4}}$ OVER $0 \leqslant x \leqslant \frac{1}{2}\pi$

N	α_1	α_2	α_3	E
1	1.0003	−0.1244	0.00330	0.00016
10	1.0000	−0.1243	0.00324	0.00006
20	1.0000	−0.1243	0.00323	0.00003
30	1.0000	−0.1243	0.00323	0.00002

(The abbreviation $E = E[u^*-u-\alpha_1(u_1^*-u_1)-\alpha_2(u_2^*-u_2)-\alpha_3(u_3^*-u_3)]$ is used.)

The results of numerical experiments are listed in table 3 for a few values of N where, in contrast with tables 1 and 2, it is observed that the relative error

$$E[u^*-u-\alpha_1(u^*-u_1)-\alpha_2(u_2^*-u_2)-\alpha_3(u_3^*-u_3)],$$

see equation (2.11), is exceedingly small even for $N=1$. Furthermore, as is discussed later, there are important practical situations where it is the amplitude of the singularity which is the prime interest and so it is worth noting here the excellent accuracy of the calculated values of the constant α_1 taken in comparison with the exact value $\alpha_1 = 1$, see equations (2.20) and (2.22).

To summarize, the kind of relations which are expressed by equations (2.23) to (2.30) are fundamental to the approach which is employed in the sequel to obtain the solution of real boundary-value problems in the presence of non-removable singularities. The approach, described by Morley (1969), makes use of the Rayleigh–Ritz method where piecewise coordinate functions u (i.e. finite elements) are supplemented with coordinate functions like the $u_1^*-u_1$, $u_2^*-u_2$, $u_3^*-u_3$ of equation (2.23).

3. PLANE HARMONIC BOUNDARY-VALUE PROBLEM

The successful treatment of a boundary-value problem presents more of a challenge than does the aforegoing solution to a one-dimensional interpolation problem where appreciable guidance is afforded by prior knowledge of the exact result.

Let us begin by examining a particular boundary-value problem which has been much investigated since its first treatment by Motz (1946) using the method of finite differences. There, the problem arose out of studies into the theory of radiation and electrostatics and requires a solution $u^*(x, y)$ to the plane harmonic field equation

$$\partial^2 u^*/\partial x^2 + \partial^2 u^*/\partial y^2 = 0 \tag{3.1}$$

over the rectangle R = OABCD which is shown in figure 1 with side lengths

$$\text{OA} = \text{AB} = \text{etc.} = 0.5.$$

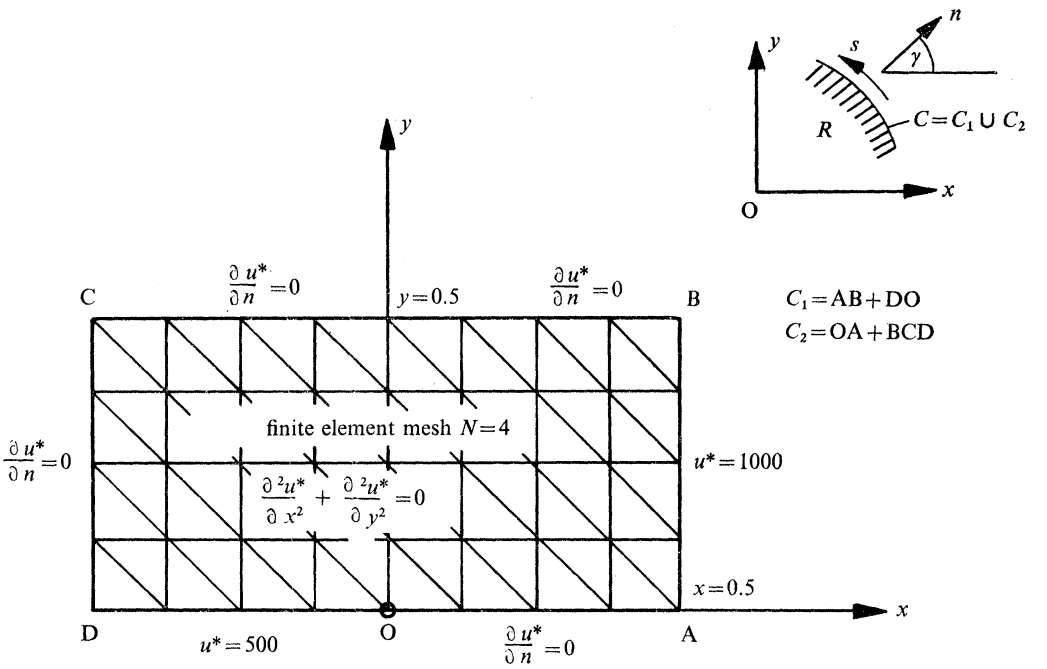

FIGURE 1. The plane harmonic problem.

The boundary is denoted by $C = C_1 \cup C_2$ and boundary conditions u^* are prescribed on C_1 according to

$$u^* = 500 \text{ on DO}, \quad u^* = 1000 \text{ on AB}, \tag{3.2}$$

and boundary conditions $\partial u^*/\partial n$ are prescribed on C_2 according to

$$\partial u^*/\partial n = 0 \text{ on OA and BCD}, \tag{3.3}$$

with the outward pointing normal n inclined at an angle γ to the Ox axis. This is known to provide a boundary-value problem with non-removable singularity at the conjunction O of the two different kinds of boundary condition.

Both Motz (1946) and Woods (1953) recognized that in order to obtain satisfactory numerical results it is necessary to provide careful treatment at the singular point. They decided to represent the behaviour near this point by special equations and then to proceed with standard finite difference equations in the more remote parts where the solution $u^*(x, y)$ is behaving smoothly enough for the use of a satisfactorily large difference interval. More recently, Whiteman has advanced a number of different solution techniques which culminate in a contribution (Whiteman 1971) to the Discussion Meeting on the uniform convergence of a finite difference solution with

mesh refinement at the singularity; the numerical values which he presented are associated with an aim to provide, in terms of accuracy and computer time, his best finite difference results so that they may be used as a benchmark by future workers. Here, the same problem is subjected to still further numerical experimentation but by the finite element method. While the results of our calculations are not wholly satisfactory they are, none the less, quite convincing when taken in comparison with Whiteman's benchmark results.

In the Rayleigh–Ritz method an approximate solution $u(x, y)$

$$u^*(x, y) \simeq u(x, y) \tag{3.4}$$

to the plane harmonic problem with exact solution $u^*(x, y)$ is obtained by minimizing the functional

$$D(u^* - u) = \iint_R \left\{ \left(\frac{\partial u^*}{\partial x} - \frac{\partial u}{\partial x} \right)^2 + \left(\frac{\partial u^*}{\partial y} - \frac{\partial u}{\partial y} \right)^2 \right\} \mathrm{d}R. \tag{3.5}$$

over the amplitudes of the set of admissible coordinate functions which make up $u(x, y)$; each of the coordinate functions must be of finite norm and the subsidiary condition

$$u = u^* \quad \text{on} \quad C_1 \tag{3.6}$$

must be satisfied. The minimum of the functional is provided by

$$\delta D(u^* - u) = -2D(u^* - u, \delta u) = 0, \tag{3.7}$$

where

$$D(u^*, u) = \iint_R \left(\frac{\partial u^*}{\partial x} \frac{\partial u}{\partial x} + \frac{\partial u^*}{\partial y} \frac{\partial u}{\partial y} \right) \mathrm{d}R = \int_C \frac{\partial u^*}{\partial n} u \, \mathrm{d}s \tag{3.8}$$

on making use of the Green formula and of equation (3.1). In a finite element application of the Rayleigh–Ritz method the coordinate functions are set up by partitioning R into, typically, triangular subregions or elements. The piecewise approximating function $u(x, y)$ is then considered to vary in a simple manner over each element with proper matching conditions along the edges. For the plane harmonic problem illustrated in figure 1, the triangular finite elements are arranged to form a uniform mesh which divides the length OA into N equally spaced intervals, the variation of $u(x, y)$ is then assumed to be linear over each element. This simple arrangement naturally imposes limitations upon the kind of problem for which a satisfactory and efficient numerical solution can be obtained. Indeed, Zlamal (1968) shows that if $u^*(x, y)$ has continuous second derivatives over R with maximum modulus M_2 and if the piecewise linear function $u(x, y)$ interpolates $u^*(x, y)$ exactly at the vertices of each triangle then, for the kind of mesh shown in figure 1,

$$|u^* - u| \leqslant 0.25 M_2 N^{-2}, \tag{3.9}$$

while the first derivatives satisfy

$$\left| \frac{\partial u^*}{\partial x} - \frac{\partial u}{\partial x} \right| \leqslant K M_2 N^{-1} \tag{3.10}$$

(cf. equation (2.15)), where K is a positive constant. It follows from equations (3.5) and (3.10) that the bound on $[D(u^* - u)]^{\frac{1}{2}}$, which gives a norm of the error, is

$$[D(u^* - u)]^{\frac{1}{2}} \leqslant K' M_2 N^{-1} \tag{3.11}$$

(cf. equation (2.17)), where K' is another positive constant. Thus, the sufficient conditions which control a satisfactory and efficient piecewise linear solution of a plane harmonic problem are similar to those encountered in the piecewise linear treatment of the one-dimensional problem of

§ 2. The best available rate of convergence requires the existence of M_2, while the accuracy is related to the actual magnitude of M_2. Consequently, in a piecewise linear finite element solution it is natural to refer to $u^*(x, y)$ as being singular whenever M_2 does not exist.

Now, the presence of a singularity at O has already been anticipated and so M_2 is known not to exist. Thus, it is not surprising to find in table 4 that there is appreciable variance between the results obtained from an ordinary finite element solution which ignores the presence of the singularity and Whiteman's (1971) benchmark results. These calculations are appropriate to a uniform mesh with size $N = 16$, cf. the relatively coarse mesh $N = 4$ which is illustrated in figure 1, and are compared in the table with Whiteman's finite difference and linear programming results at points near to the singularity along the line OA, i.e. $y = 0$.

TABLE 4. RESULTS FROM ORDINARY FINITE ELEMENT SOLUTION $u^* \simeq u$ TO THE PLANE HARMONIC PROBLEM

	values of $u^* \simeq u$ along $y = 0$ at				
	$x = 0$	$x = \mathrm{OA}/28$	$x = \mathrm{OA}/14$	$x = 3\mathrm{OA}/28$	$x = \mathrm{OA}/17$
f.e. mesh, $N = 16$	500	547.35	590.04	618.78	644.11
Whiteman (1971), f.d.	500	573.0	606.6	632.7	655.0
Whiteman (1971), l.p.	500	576.4	608.9	634.5	656.5

The following abbreviations are used: f.e., finite element; f.d., finite difference; l.p., linear programming.

This further evidence amplifies the need to take proper account of the singular behaviour. Thus, as in equation (2.22), we begin by seeking a suitable expansion for $u^*(x, y)$,

$$u^*(x, y) \simeq 500 + \alpha_1 u_1^*(x, y) + \alpha_2 u_2^*(x, y) + \ldots, \tag{3.12}$$

with the intention of reproducing the analytic structure at the singular point $x = 0, y = 0$. While determination of the magnitudes of the (real) constants $\alpha_1, \alpha_2, \ldots$ has to be left until the closing stages of the calculations, immediate attention needs to be given to a suitable form for the functions $u_1^*(x, y), u_2^*(x, y), \ldots$. Many formally equivalent forms are available, but the specific choice is of special importance to the successful outcome of a practical calculation. Thus, the opportunity is taken, in dealing with what is after all a relatively simple boundary-value problem, to examine the numerical outcome of taking two different forms for these functions.

3.1. *First singular solution; exact satisfaction of all subsidiary conditions*

The plane harmonic functions $\tilde{u}_j^*(x, y)$

$$\tilde{u}_j^*(x, y) = -\mathrm{Re}\, 2z^{j-\frac{1}{2}} \quad (j = 1, 2, 3, \ldots), \tag{3.13}$$

satisfy the field equation (3.1) with z the complex variable

$$z = x + iy \tag{3.14}$$

and Re denoting that the real part is to be taken. These functions have finite norm, see equation (3.5), and satisfy boundary conditions

$$\left.\begin{aligned} \tilde{u}_j^* &= 0 \quad \text{for} \quad x \leqslant 0, \quad y = 0, \quad \text{i.e. along DO,} \\ \partial \tilde{u}_j^*/\partial n &= 0 \quad \text{for} \quad x > 0, \quad y = 0, \quad \text{i.e. along OA.} \end{aligned}\right\} \tag{3.15}$$

Since both field equation and homogeneous boundary conditions are satisfied adjacent to $x = 0$, $y = 0$ we conclude that this set of functions $\tilde{u}_j^*(x, y)$ is adequate to reproduce the analytic structure

of the singularity. Moreover, in accordance with our earlier definition, the equation (3.13) reveals the existence of a nested double singularity because bounded second derivatives M_2 do not exist for $j = 1, 2$. The remaining terms in the set are characterized as supplementary and, in view of the experience with the one-dimensional problem, the first few terms are retained in the hope of reducing the influence of large magnitudes of second derivatives that may occur in R away from the singular point. The branch which is to be taken for the square root in equation (3.13) is such that, for $j = 1$,

$$\lim_{\substack{x\to 0^- \\ y=0}} |x^{\frac{1}{2}}|\,\partial \tilde{u}_1^*/\partial y = 1. \tag{3.16}$$

The exact satisfaction of all subsidiary conditions on C_1, see equations (3.6) and (3.2), requires further that the $u_j^*(x, y)$ of equation (3.12) have at most a piecewise linear variation along AB, i.e. along $x = 0.5$. To this effect, note that the harmonic functions

$$2\mathrm{i}(z-0.5)\,(z-1)^{j-\frac{1}{2}} \quad (j = 1, 2, 3, \ldots) \tag{3.17}$$

possess derivatives of all orders which are continuous in R and are non-zero at $x = 0, y = 0$. Thus, the essential qualities which are enjoyed by equation (3.13) remain unchanged if we put

$$u_j^*(x, y) = -\mathrm{Re}\,2\mathrm{i}(z-0.5)\,(z-1)^{j-\frac{1}{2}}\,(2z^{j-\frac{1}{2}}) \quad (j = 1, 2, 3, \ldots). \tag{3.18}$$

This form is, at first sight, commendable because each $u_j^*(x, y)$ now satisfies homogeneous subsidiary conditions along the whole of C_1, namely

$$\left.\begin{aligned} u_j^* &= 0 \quad \text{for} \quad x \leqslant 0, \quad y = 0, \quad \text{i.e. along DO,} \\ u_j^* &= 0 \quad \text{for} \quad x = 0.5, \quad y \geqslant 0, \quad \text{i.e. along AB,} \end{aligned}\right\} \tag{3.19}$$

as well as satisfying on the part of C_2 adjacent to the singular point the condition

$$\partial u_j^*/\partial n = 0 \quad \text{for} \quad x > 0, \quad y = 0, \quad \text{i.e. along OA.} \tag{3.20}$$

It is remarked that it is only in rather exceptional practical situations that such $u_j^*(x, y)$ constitute, as in equation (3.18), intrinsically admissible coordinate functions for the Rayleigh–Ritz method.

We may now proceed similarly as in the one-dimensional problem, see equations (2.23) *et seq.* Thus, instead of equation (3.4) put

$$u^* \simeq u + \alpha_1(u_1^* - u_1) + \alpha_2(u_2^* - u_2) + \ldots, \tag{3.21}$$

where $u_1^*(x, y), u_2^*(x, y), \ldots$ are defined by equation (3.18) and where $u(x, y), u_1(x, y), u_2(x, y), \ldots$ are continuous piecewise linear functions each taken over the same finite element mesh with $\alpha_1, \alpha_2, \ldots$ as arbitrary constants. Next, minimize the functional of equation (3.5),

$$D[u^* - u - \alpha_1(u_1^* - u_1) - \alpha_2(u_2^* - u_2) - \ldots] \tag{3.22}$$

subject to the satisfaction of subsidiary conditions, see equations (3.2), (3.6) and (3.19),

$$u = u^*, \quad u_j = u_j^* \quad (j = 1, 2, 3, \ldots) \text{ on } C_1, \tag{3.23}$$

where the nodal values of all the piecewise linear functions, as well as the constants $\alpha_1, \alpha_2, \ldots$, are to be subjected to arbitrary variation. As in the one-dimensional problem, the minimization of the functional requires that

$$\delta D(u^* - u) = \delta D(u_1^* - u_1) = \delta D(u_2^* - u_2) = \ldots = 0, \tag{3.24}$$

subject to the satisfaction of the subsidiary conditions. Again, $u(x, y)$ is found to be identical with the ordinary finite element solution to $u^*(x, y)$ while $u_1(x, y), u_2(x, y), \ldots$ are found to be the ordinary finite element solutions respectively to $u_1^*(x, y), u_2^*(x, y), \ldots$ without regard having been given to the behaviour near the singular point. Moreover, all these finite element solutions can be calculated simultaneously because of the complete identity in each instance between the associated band matrices. The constants $\alpha_1, \alpha_2, \ldots$ are subsequently calculated from simultaneous linear equations like (2.29) but here, in virtue of equations (3.8), (3.19), (3.23) and (3.24),

$$D(u_j^* - u_j, u_k^* - u_k) = \int_{C_2} \frac{\partial u_k^*}{\partial n} (u_j^* - u_j)\, \mathrm{d}s \quad (j, k = 1, 2, 3, \ldots) \tag{3.25}$$

and, with the further help of equation (3.3),

$$D(u_j^* - u_j, u^* - u) = -\int_C \frac{\partial u_j^*}{\partial n} u\, \mathrm{d}s \quad (j = 1, 2, 3, \ldots). \tag{3.26}$$

It is worth drawing attention to the simplicity of this application of the modified Rayleigh–Ritz method; it requires evaluation of the functions $u_j^*(x, y)$ and normal derivatives $\partial u_j^*/\partial n$ only on the boundary C.

A few numerical results are listed in table 5 for various sizes of finite element meshes. The available computer program accommodates up to four functions of the type $u_j^*(x, y)$ and so the series in equation (3.21) is truncated accordingly. The results are listed for points which are near to the singularity and, although they are in closer agreement than the ordinary finite element

TABLE 5. RESULTS FROM FIRST SINGULAR SOLUTION

$$u^* \simeq u + \alpha_1(u_1^* - u_1) + \alpha_2(u_2^* - u_2) + \alpha_3(u_3^* - u_3) + \alpha_4(u_4^* - u_4)$$

TO THE PLANE HARMONIC PROBLEM

	values of $u^* \simeq u + \alpha_1(u_1^* - u_1)$ ... along $y = 0$ at				
	$x = 0$	$x = \mathrm{OA}/28$	$x = \mathrm{OA}/14$	$x = 3\mathrm{OA}/28$	$x = \mathrm{OA}/7$
f.e. mesh, $N = 4$	500	554.30	584.98	611.16	634.78
5	500	558.09	589.85	616.60	640.50
6	500	560.97	593.47	620.54	644.53
10	500	567.69	601.45	628.65	651.71
14	500	570.90	604.91	631.35	653.79
15	500	571.44	605.38	631.72	654.24
16	500	571.92	605.78	632.03	654.57
Whiteman (1971), f.d.	500	573.0	606.6	632.7	655.0
Whiteman (1971), l.p.	500	576.4	608.9	634.5	656.5

The following abbreviations are used: f.e., finite element; f.d., finite difference; l.p., linear programming.

TABLE 6. COEFFICIENTS α_1, α_2, α_3, α_4 FROM FIRST SINGULAR SOLUTION

TO THE PLANE HARMONIC PROBLEM

	α_1	$N^{0.595}(\alpha_1 + 304.44)$	α_2	$N^{0.575}(\alpha_2 - 80.38)$	α_3	$N^{0.545}(\alpha_3 + 36.69)$	α_4	$N^{0.535}(\alpha_4 - 8.11)$
e. mesh, $N = 4$	−142.87	368.63	38.03	−93.99	−20.07	35.38	4.36	−7.46
5	−159.23	378.33	42.09	−96.62	−21.51	36.48	4.68	−7.89
6	−172.23	383.93	45.36	−98.13	−22.71	37.11	4.94	−8.13
10	−205.16	390.71	53.80	−99.93	−25.90	37.85	5.65	−8.43
14	−223.09	391.08	58.45	−100.03	−27.70	37.89	6.06	−8.43
15	−226.37	391.07	59.31	−100.03	−28.03	37.88	6.13	−8.43
16	−229.31	391.08	60.07	−100.03	−28.33	37.89	6.20	−8.43

results of table 4 with Whiteman's (1971) benchmark results, they are not convincing because of the substantial changes which occur during the advance to finer meshes. The nature of these changes becomes more apparent after examination of table 6 which gives magnitudes of the constants α_1, α_2, α_3, α_4 for various mesh sizes N. Similarly, to equation (2.13) it is observed, for the finer mesh sizes, that the behaviour of these α may be closely approximated by

$$\alpha \simeq \alpha'(1+cN^{-\gamma}), \tag{3.27}$$

where α' is the extrapolation of α for very large values of N, while the magnitude of the modulus of c indicates whether the solution is satisfactory for small values of N, and γ measures the rate of convergence. In the most favourable circumstances one might expect $\gamma = 2$, for a piecewise linear solution, and $|c| \ll 1$. From table 6, we find

$$\left.\begin{aligned} \alpha_1 &= -304.44(1-1.285N^{-0.595}) = -229.31 \text{ for } N = 16,\\ \alpha_2 &= 80.38(1-1.244N^{-0.575}) = 60.07 \text{ for } N = 16,\\ \alpha_3 &= -36.69(1-1.033N^{-0.545}) = -28.33 \text{ for } N = 16,\\ \alpha_4 &= 8.11(1-1.039N^{-0.535}) = 6.20 \text{ for } N = 16, \end{aligned}\right\} \tag{3.28}$$

and this reveals markedly inferior-rates of convergence γ as well as unacceptably large values of c. (It is of interest to note here that the finite difference calculations by Motz (1946) and Woods (1953) provide values $\alpha_1 = -285.6$ and $\alpha_1 = -304$ respectively.) Furthermore, the substitution of equations (3.18) and (3.28) into the truncated equation (3.12) should, as originally intended, reproduce accurately the behaviour near the singular point, say at $x = \mathrm{OA}/28$, $y = 0$. Typically for the finite element mesh $N = 16$ we have

$$\left.\begin{aligned} u^*(x,y) &\simeq 500 - 229.31u_1^*(x,y) + 60.07u_2^*(x,y)\\ &\quad - 28.33u_3^*(x,y) + 6.20u_4^*(x,y)\\ &= 558.84 \quad \text{at} \quad x = \tfrac{1}{28}\mathrm{OA}, \quad y = 0, \end{aligned}\right\} \tag{3.29}$$

and this value compares unsatisfactorily with the 571.92 listed in table 5. These results are considered quite unacceptable and the disparities are attributed to the form chosen in equation (3.18) to represent the functions $u_j^*(x,y)$.

3.2. *Second singular solution; approximate satisfaction of subsidiary conditions*

The finite element method shares with the finite difference method the powerful capability of satisfying, in a piecewise sense, arbitrary subsidiary conditions. In the present context this means that advantage can be taken of the simpler form,

$$u_j^*(x,y) = \tilde{u}_j^*(x,y) = -\operatorname{Re} 2z^{j-\frac{1}{2}} \quad (j = 1, 2, 3, \ldots) \tag{3.30}$$

for the functions $u_j^*(x,y)$ (see equation (3.13)) instead of that given by equation (3.18) which is now suspect because of the constraint it may impose on the accurate representation of the analytic structure at the nested singularity.

This second solution to the boundary-value problem proceeds in the same manner as in equations (3.21) *et seq.* except that in equation (3.23) the subsidiary conditions $u_j = u_j^*$ are satisfied exactly here only at the nodal points along the part AB of the boundary C_1. This part of the boundary is, incidentally, far removed from the singularity so that the functions $u_j^*(x,y)$ are varying relatively slowly.† These subsidiary conditions are no longer homogeneous and a conse-

† These subsidiary conditions can be satisfied exactly by abandoning the linear variation of $u_j(x,y)$ along those triangular finite element sides which have union with C_1. This requires, however, slightly differing coordinate functions for each of $u(x,y)$, $u_j(x,y)$ with the result that deductions like those of equation (2.27) are not then strictly valid.

quence is that equations (3.25) and (3.26) have to be modified to

$$D(u_j^* - u_j, u_k^* - u_k) \simeq \int_{C_2} \frac{\partial u_k^*}{\partial n}(u_j^* - u_j)\,\mathrm{d}s - \int_{C_1} \frac{\partial u_j^*}{\partial n} u_k \mathrm{d}s + D(u_j, u_k^0), \tag{3.31}$$

where u_k^0 is a piecewise linear function taken over the finite element mesh such that

$$\left.\begin{aligned} u_k^0 &= u_k^* \quad \text{at nodes on } C_1, \\ u_k^0 &= 0 \quad \text{at all other nodes,} \end{aligned}\right\} \tag{3.32}$$

and

$$D(u_j^* - u_j, u^* - u) \simeq -\int_{C_1} \frac{\partial u_j^*}{\partial n} u\,\mathrm{d}s + D(u_j, u^0); \tag{3.33}$$

similarly, for the piecewise linear function u^0 where

$$\left.\begin{aligned} u^0 &= u^* \quad \text{at nodes on } C_1, \\ u^0 &= 0 \quad \text{at all other nodes.} \end{aligned}\right\} \tag{3.34}$$

Approximations which are involved in equations (3.31) and (3.33) arise out of the aforementioned inexact satisfaction of subsidiary conditions between the nodal points on the part AB of C_1. The $D(u_j, u_k^0)$, $D(u_j, u^0)$ are very simple to calculate in virtue of equations (3.32) and (3.34) while the remaining quantities again require evaluation of the functions $u_j^*(x, y)$ and normal derivatives $\partial u_j^*/\partial n$ only on the boundary C.

Some numerical results for points near the singularity are presented in table 7 for the same finite element meshes as are used for the first singular solution. Equation (3.21), this time with substitutions from equation (3.30), is again truncated after the fourth term. The convergence is now more convincing with quite accurate values from the very coarse finite element mesh $N = 4$.

TABLE 7. RESULTS FROM SECOND SINGULAR SOLUTION

$$u^* \simeq u + \alpha_1(u_1^* - u_1) + \alpha_2(u_2^* - u_2) + \alpha_3(u_3^* - u_3) + \alpha_4(u_4^* - u_4)$$

TO THE PLANE HARMONIC PROBLEM

	values of $u^* \simeq u + \alpha_1(u_1^* - u_1)$ ... along $y = 0$ at				
	$x = 0$	$x = \mathrm{OA}/28$	$x = \mathrm{OA}/14$	$x = 3\mathrm{OA}/28$	$x = \mathrm{OA}/7$
f.e. mesh, $N = 4$	500	577.13	609.80	635.38	657.35
5	500	576.89	609.45	634.94	656.85
6	500	576.73	609.23	634.67	656.54
10	500	576.44	608.83	634.24	656.25
14	500	576.33	608.68	634.17	656.13
15	500	576.31	608.68	634.15	656.13
16	500	576.29	608.67	634.14	656.12
Whiteman (1971), f.d.	500	573.0	606.6	632.7	655.0
Whiteman (1971), l.p.	500	576.4	608.9	634.5	656.5

The following abbreviations are used: f.e., finite element; f.d., finite difference; l.p., linear programming.

A comprehensive comparison with Whiteman's benchmark results, both from the finite difference and linear programming calculations, is provided in figure 2 for points near to and surrounding the singularity for the fine finite element meshes $N = 15$ and $N = 16$. In all instances these finite element results are bounded by those of Whiteman and are in closest agreement with his linear programming results; the largest-variation between finite element results from the meshes $N = 15$ and $N = 16$ amounts here to less than 0.003 %. A more critical analysis of the validity of

these finite element results is provided from an examination of table 8 which lists the magnitudes of the constants $\alpha_1, \alpha_2, \alpha_3, \alpha_4$ for various mesh sizes N. For the finer meshes the behaviour is seen to be like

$$\left.\begin{aligned} \alpha_1 &= -282.70(1+0.053N^{-0.930}) = -283.84 \quad \text{for} \quad N = 16, \\ \alpha_2 &= -127.69(1-1.540N^{-1.592}) = -125.31 \quad \text{for} \quad N = 16, \\ \alpha_3 &= 56.43(1+0.536N^{-1.620}) = 56.77 \quad \text{for} \quad N = 16, \\ \alpha_4 &= 156.80(1-1.124N^{-1.264}) = 151.50 \quad \text{for} \quad N = 16. \end{aligned}\right\} \tag{3.35}$$

All four rates of convergence γ (see equation (3.27)) are substantial improvements upon those of equation (3.28) for the first singular solution. While the value attained by $|c|$ (see equation (3.27)) is acceptable in respect of the dominant term α_1, the values which are attained by the remaining terms are disappointingly large. Substituting equations (3.30) and (3.35) into the

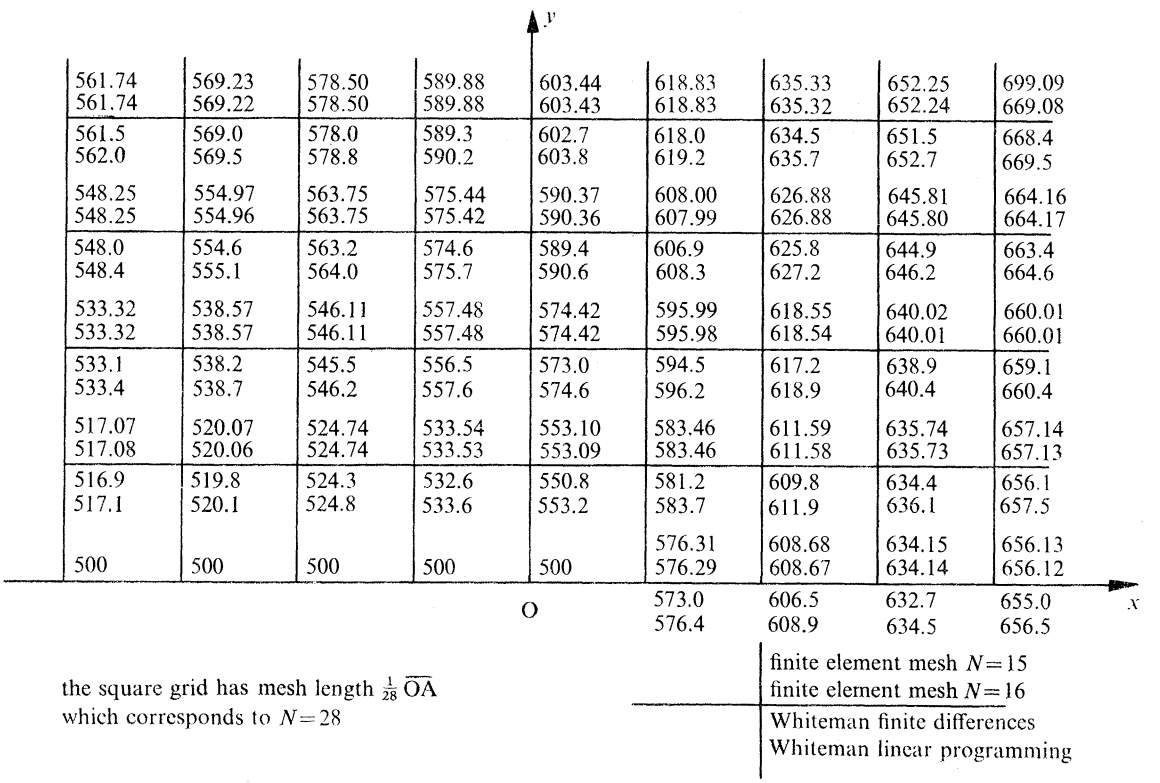

FIGURE 2. Comparative results for plane harmonic problem, second singular solution.

TABLE 8. COEFFICIENTS $\alpha_1, \alpha_2, \alpha_3, \alpha_4$ FROM SECOND SINGULAR SOLUTION TO THE PLANE HARMONIC PROBLEM

	α_1	$N^{0.930}(\alpha_1+282.70)$	α_2	$N^{1.592}(\alpha_2+127.69)$	α_3	$N^{1.620}(\alpha_3-56.43)$	α_4	$N^{1.264}(\alpha_4-156.80)$
mesh $N=4$	−286.71	−14.58	−110.17	159.17	59.34	27.41	126.21	−176.41
5	−286.00	−14.77	−114.15	175.50	58.55	28.68	132.60	−185.04
6	−285.51	−14.91	−117.02	184.88	58.05	29.38	137.36	−187.16
10	−284.47	−15.09	−122.67	196.06	57.16	30.19	146.95	−180.73
14	−283.99	−15.10	−124.74	196.64	56.85	30.22	150.52	−176.31
15	−283.91	−15.10	−125.05	196.63	56.81	30.22	151.05	−176.14
16	−283.84	−15.10	−125.31	196.64	56.77	30.22	151.50	−176.31

truncated equation (3.12) provides, for the finite element mesh $N = 16$,

$$\left.\begin{aligned} u^*(x,y) &\simeq 500 - 283.84u_1^*(x,y) - 125.31u_2^*(x,y) + 56.77u_3^*(x,y) + 151.50u_4^*(x,y) \\ &= 576.45 \text{ at } x = \tfrac{1}{28}\text{OA}, \quad y = 0, \end{aligned}\right\} \tag{3.36}$$

and this value compares favourably with the 576.29 listed in table 7.† Our conclusion is that although the numerical results for this second singular solution are likely to be acceptable in most practical situations they are not wholly satisfactory because of the deficiencies as revealed by equations (3.35). The matter is pursued no further here but the remedy apparently lies in still further adjustments to the forms, equations (3.18) and (3.30), which are selected for the functions $u_j^*(x,y)$. The situation is typical of ordinary applications of the Rayleigh–Ritz method when resource is made to additional, or different, coordinate functions to effect an improved solution.

4. Plane stress elasticity boundary-value problems

Singular effects occur over a wide range of different situations in elastic plane stress, see, for example, Morley (1963), but attention is specific here to cracked plates with the purpose of illustrating the manner of calculation for an engineering assessment of the stress intensity factor. As explained in the Introduction, this class of problem occurs in fracture mechanics where prediction of safety is based upon the amplitude of the dominant stress singularity, i.e. the stress intensity factor. The more classical methods of calculation are treated in the book by Sneddon & Lowengrub (1969), while Wilson (1969) and Newman (1971) have made extensive use of collocation techniques. In the finite element method the displacement 'super element' approach is typified by the work of Byskov (1970) while Pian, Tong & Luk (1971) employ a mixed variational approach as a way to overcome the difficulties of inter-element displacement continuity and allow the singular functions to range over several elements. Consequently, it is not surprising to find that no attempt is made in such approaches to maintain continuity of the first, let alone the second, derivatives of the displacements; furthermore, considerations of relative sizing of the singular regions are also largely unresolved. The numerical examples which we have already treated indicate that such factors can be responsible for serious degradation in the achieved accuracy and may, in any case, be avoided in a solution by the present method.

The displacements u_x^*, u_y^*, in an isotropic elastic plate in plane stress are governed, in the absence of surface forces, by the simultaneous field equations

$$\left.\begin{aligned} \frac{\partial^2 u_x^*}{\partial x^2} + \tfrac{1}{2}(1-\nu)\frac{\partial^2 u_x^*}{\partial y^2} + \tfrac{1}{2}(1+\nu)\frac{\partial^2 u_y^*}{\partial x \partial y} &= 0, \\ \tfrac{1}{2}(1+\nu)\frac{\partial^2 u_x^*}{\partial x \partial y} + \frac{\partial^2 u_y^*}{\partial y^2} + \tfrac{1}{2}(1-\nu)\frac{\partial^2 u_y^*}{\partial x^2} &= 0, \end{aligned}\right\} \tag{4.1}$$

† In several practical situations it is only the values of the $\alpha_1, \alpha_2, \ldots$, which are of interest. Equations (3.36) indicate that good estimates of these values may be readily obtained by simple devices, like minimizing

$$D'(u - 500 - \alpha_1 u_1 - \alpha_2 u_2 \ldots)$$

with respect to $\alpha_1, \alpha_2 \ldots$ where

$$D'(u, u_1) = \int\int_{R'} \left(\frac{\partial u}{\partial x}\frac{\partial u_1}{\partial x} + \frac{\partial u}{\partial y}\frac{\partial u_1}{\partial y}\right) \mathrm{d}R'$$

with R' a small region which is suitably contracted around the singular point.

where ν is the Poisson ratio. The stress–displacement relations are

$$\sigma_x^* = \frac{E}{1-\nu^2}(e_x^* + \nu e_y^*), \quad \sigma_y^* = \frac{E}{1-\nu^2}(e_y^* + \nu e_x^*), \quad \tau_{xy}^* = \frac{E}{2(1+\nu)}\gamma_{xy}^*, \tag{4.2}$$

where the strain components are defined by

$$e_x^* = \partial u_x^*/\partial x, \quad e_y^* = \partial u_y^*/\partial y, \quad \gamma_{xy}^* = \partial u_x^*/\partial y + \partial u_y^*/\partial x \tag{4.3}$$

and E is the Young modulus. On the boundary $C = C_1 \cup C_2$ (see figure 3) the normal and tangential displacements are described respectively by

$$u_n^* = u_x^* \cos\gamma + u_y^* \sin\gamma, \quad u_s^* = -u_x^* \sin\gamma + u_y^* \cos\gamma, \tag{4.4}$$

with corresponding tractions

$$\left.\begin{aligned} \sigma_n^* &= \sigma_x^* \cos^2\gamma + \sigma_y^* \sin^2\gamma + 2\tau_{xy}^* \sin\gamma\cos\gamma, \\ \tau_{ns}^* &= -(\sigma_x^* - \sigma_y^*)\sin\gamma\cos\gamma + \tau_{xy}^*(\cos^2\gamma - \sin^2\gamma), \end{aligned}\right\} \tag{4.5}$$

with n the outwards pointing normal inclined at an angle γ to the Ox axis and s measured around the enclosing boundary C in the positive anticlockwise direction.

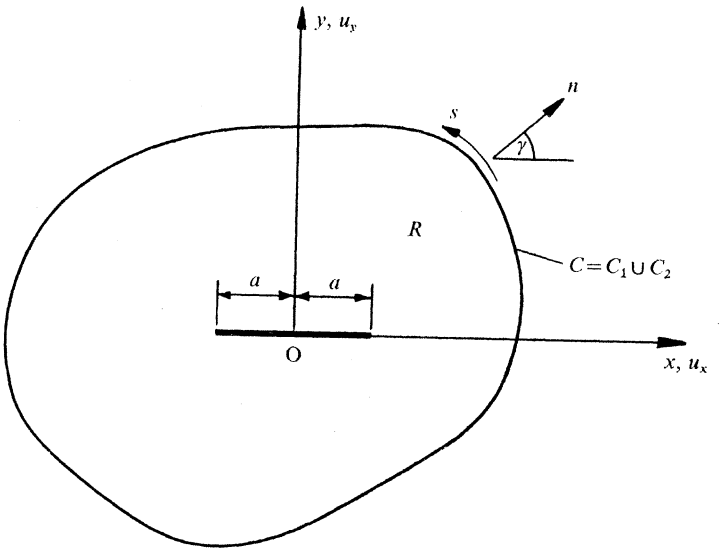

Kinematic boundary conditions u_n^* and/or u_s^* are prescribed on C_1.
Traction boundary conditions σ_n^* and/or τ_{ns}^* are prescribed on C_2.

FIGURE 3. Notation for plane stress elasticity problem with crack.

It is convenient to denote the approximate solution $u_x(x, y)$, $u_y(x, y)$ where

$$u_x^*(x, y) \simeq u_x(x, y), \quad u_y^*(x, y) \simeq u_y(x, y) \tag{4.6}$$

to the simultaneous field equations (4.1) by the symbolic representation

$$u^*(x, y) \simeq u(x, y). \tag{4.7}$$

Thus, in the Rayleigh–Ritz method an approximate solution $u(x, y)$ is obtained by minimizing the functional

$$D(u^* - u) = \iint_R [(\sigma_x^* - \sigma_x)(e_x^* - e_x) + (\sigma_y^* - \sigma_y)(e_y^* - e_y) + (\tau_{xy}^* - \tau_{xy})(\gamma_{xy}^* - \gamma_{xy})]\, dR \tag{4.8}$$

over the amplitudes of the set of admissible coordinate functions which make up $u(x, y)$; each coordinate function must be of finite norm and the subsidiary conditions

$$u_n = u_n^* \quad \text{and/or} \quad u_s = u_s^* \quad \text{on} \quad C_1 \tag{4.9}$$

must be satisfied. The stresses and strains σ_x, e_x, etc. are calculated by substituting $u_x(x, y)$, $u_y(x, y)$ appropriately into equations (4.2) and (4.3). The minimum of the functional is provided by

$$\delta D(u^* - u) = -2D(u^* - u, \delta u) = 0, \tag{4.10}$$

where

$$\left.\begin{aligned} D(u^*, u) &= \iint_R (\sigma_x^* e_x + \sigma_y^* e_y + \tau_{xy}^* \gamma_{xy})\, \mathrm{d}R \\ &= \int_C (\sigma_n^* u_n + \tau_{ns}^* u_s)\, \mathrm{d}s \end{aligned}\right\} \tag{4.11}$$

on making use of the Green formula and of equations (4.1) to (4.5).

As in the previous problems the piecewise approximating displacements $u(x, y)$ are assumed to vary linearly over each of the triangular elements which constitute the finite element mesh; likewise, it can then be shown that to achieve the best available rate of convergence requires the existence of bounded second derivatives, with maximum modulus M_2, for the exact solution $u^*(x, y)$. In solving the problem of a cracked plate we thus seek an expansion for $u^*(x, y)$ in the form

$$\left.\begin{aligned} u_x^*(x, y) &\simeq \alpha x + \sum_{k=1} \alpha_k u_{xk}^*(x, y), \\ u_y^*(x, y) &\simeq -\alpha \nu y + \sum_{k=1} \alpha_k u_{yk}^*(x, y), \end{aligned}\right\} \tag{4.12}$$

with the intention of reproducing the analytic structure, apart from possible rigid body movements, of the behaviour in the neighbourhood of the crack tips. The magnitudes of the constants α_k are to be determined by the modified Rayleigh–Ritz method, whereas the constant α may be left undetermined in a piecewise linear solution for the displacements.

4.1. *Singular functions for crack problems*

The general solution for the displacements u_x^*, u_y^* which are governed by the simultaneous field equations (4.1) is derived in complex variable form by Muskhelishvili (1953). It may be written

$$u_x^* + \mathrm{i}u_y^* = \frac{1}{E}\{(3 - \nu)\, \phi(z) - (1 + \nu)\, [\omega(\bar{z}) + (z - \bar{z})\, \overline{\phi'(z)}]\}, \tag{4.13}$$

where $\phi(z)$, $\omega(z)$ are arbitrary regular functions inside the region R of the complex variable

$$z = x + \mathrm{i}y. \tag{4.14}$$

The bar indicates the complex conjugate and the prime indicates differentiation with respect to the complex variable. The stresses acting in a plate of unit thickness are then given by

$$\left.\begin{aligned} \sigma_x^* + \sigma_y^* &= 2[\phi'(z) + \overline{\phi'(z)}], \\ \sigma_y^* - \mathrm{i}\tau_{xy}^* &= \phi'(z) + \omega'(\bar{z}) + (z - \bar{z})\, \overline{\phi''(z)}. \end{aligned}\right\} \tag{4.15}$$

Consider now the single-valued functions

$$\left.\begin{aligned} \phi_j(z) &= \omega_j(z) = [(z^2 - a^2)/2a]^{\frac{1}{2}} F_j(z/a) \\ \phi_{j+1}(z) &= \omega_{j+1}(z) = -\mathrm{i}\phi_j(z) \end{aligned}\right\} \quad (j = 1, 3, 5, \ldots), \tag{4.16}$$

where

$$\left.\begin{aligned} F_1(z) &= 1, & F_7(z) &= z(z^2-1), \\ F_3(z) &= z, & F_9(z) &= (z^2-1)^2, \\ F_5(z) &= z^2-1, & &\ldots \end{aligned}\right\} \tag{4.17}$$

appropriate to a crack of length $2a$ with centre at O and lying along the Ox coordinate axis as shown in figure 3. When these functions are substituted into equations (4.13), (4.15) and (4.3) they yield expressions for the stresses and strains which give finite norm for the functional of equation (4.8). The stresses σ^*_{yj} and τ^*_{xyj} acting along the Ox coordinate axis are then obtained from the second of equations (4.15) with $z = \bar{z} = x$ as follows

$$\left.\begin{aligned} \sigma^*_{yj} &= \tau^*_{xy(j+1)} = 2[xF_j(x/a) + (x^2-a^2)\,F_j'(x/a)]\,\mathrm{Re}[(x^2-a^2)\,2a]^{-\frac{1}{2}} \\ \sigma^*_{y(j+1)} &= \tau^*_{xyj} = 0 \end{aligned}\right\} \quad (j = 1, 3, 5, \ldots). \tag{4.18}$$

Thus, from equations (4.5), the tractions satisfy the required boundary conditions

$$\sigma^*_{nk} = \tau^*_{nsk} = 0 \quad \text{for} \quad -a < x < a, \quad y = 0, \tag{4.19}$$

i.e. along the crack face, for all k. Moreover, we may select the branch for the square root in equation (4.16) such that the 'stress intensity' at the crack tip $x = a^+$, $y = 0$ is given by

$$\left.\begin{aligned} \lim_{\substack{x\to a^+ \\ y=0}} |(x-a)^{\frac{1}{2}}|\,\sigma^*_{yk} = \lim_{\substack{x\to a+ \\ y=0}} |(x-a)^{\frac{1}{2}}|\,\tau^*_{xy(k+1)} &= 1, \quad k = 1, 3, \\ &= 0, \quad k \neq 1, 3. \end{aligned}\right\} \tag{4.20}$$

The equations (4.13) and (4.16), (4.17) indicate, in the context of a piecewise linear solution, that a total of eight singularities are properly to be associated with a crack because of the unboundedness at the crack tips $x = \pm a$, $y = 0$ of the second derivatives of the $\phi_k(z)$, $\omega_k(z)$ for $k = 1, 2, 3, \ldots, 8$.

In the modified Rayleigh–Ritz method we put, instead of equation (4.7),

$$u^* \simeq u + \sum_{k=1} \alpha_k(u^*_k - u_k), \tag{4.21}$$

where the $u^*_k(x, y)$ are obtained by substituting equations (4.16) into (4.13) and where $u(x, y)$, $u_k(x, y)$ are continuous piecewise linear functions each taken over the same finite element mesh. The series is to be truncated in the knowledge that a satisfactory solution properly requires retention of at least the first eight terms which involve the constants α_k. Moreover, equations (4.20) show that the first four constants α_k are direct measures of the stress intensity factors. The functional of equation (4.8), with new argument

$$D[u^* - u - \sum_{k=1} \alpha_k(u^*_k - u_k)] \tag{4.22}$$

is now minimized subject to the subsidiary conditions, see equations (4.9),

$$\left.\begin{aligned} u_n &= u^*_n \\ u_{nk} &= u^*_{nk} \end{aligned}\right\} \quad \text{and/or} \quad \left.\begin{aligned} u_s &= u^*_s \\ u_{sk} &= u^*_{sk} \end{aligned}\right\} \quad \text{on } C_1 \quad (k = 1, 2, 3, \ldots) \tag{4.23}$$

being satisfied at least at the finite element mesh node points which lie on C_1. If the consequences of errors arising from pointwise satisfaction of the subsidiary conditions are ignored, the minimization of equation (4.22) provides individual equations

$$\delta D(u^* - u) = \delta D(u^*_k - u_k) = 0 \quad (k = 1, 2, 3, \ldots), \tag{4.24}$$

where the variations are arbitrary subject to the satisfaction of equations (4.23). Thus, $u(x, y)$ is identical with the ordinary finite element solution to $u^*(x, y)$, while the $u_k(x, y)$ are the ordinary finite element solutions to the $u_k^*(x, y)$ without regard having been given to the singular behaviours; all these finite element solutions may be calculated simultaneously. The constants α_k are subsequently calculated from simultaneous linear equations like (2.29) where here, in virtue of equations (4.11), (4.23) and (4.24),

$$D(u_j^* - u_j, u_k^* - u_k) \simeq \int_{C_2} [\sigma_{nk}^*(u_{nj}^* - u_{nj}) + \tau_{nsk}^*(u_{sj}^* - u_{sj})]\, \mathrm{d}s - \int_{C_1} (\sigma_{nj}^* u_{nk} + \tau_{nsj}^* u_{sk})\, \mathrm{d}s + D(u_j, u_k^0), \tag{4.25}$$

where u_k^0 represents piecewise linear functions taken over the finite element mesh such that

$$\left.\begin{aligned} u_{nk}^0 = u_{nk}^* \quad \text{and/or} \quad u_{sk}^0 = u_{sk}^* \quad \text{at nodes on } C_1, \\ u_{xk}^0 = u_{yk}^0 = 0 \quad \text{at all other nodes,} \end{aligned}\right\} \tag{4.26}$$

and

$$D(u_j^* - u_j, u^* - u) \simeq \int_{C_2} [\sigma_n^*(u_{nj}^* - u_{nj}) + \tau_{ns}^*(u_{sj}^* - u_{sj})]\, \mathrm{d}s - \int_{C_1} (\sigma_{nj}^* u_n + \tau_{nsj}^* u_s)\, \mathrm{d}s + D(u_j, u^0), \tag{4.27}$$

similarly, with u^0 representing piecewise linear functions where

$$\left.\begin{aligned} u_n^0 = u_n^* \quad \text{and/or} \quad u_s^0 = u_s^* \quad \text{at nodes on } C_1, \\ u_x^0 = u_y^0 = 0 \quad \text{at all other nodes.} \end{aligned}\right\} \tag{4.28}$$

Any approximations which may be involved in equations (4.25) and (4.27) arise out of pointwise satisfaction of the subsidiary conditions in equations (4.23).

In virtue of the fact that the singular functions $u_k^*(x, y)$ satisfy the homogeneous field equations (4.1) throughout the whole of R it is necessary to evaluate the $u_k^*(x, y)$ and first derivatives only on the boundary C. However, there may occur in practice other more compelling reasons, such as where the plate is part of an extensive structure with multiple reinforcements, to adapt Fix's (1969) idea, to the modified Rayleigh–Ritz method in order to localize the range of the singular functions $u_k^*(x, y)$. In such cases it is necessary to evaluate the $u_k^*(x, y)$ and first derivatives at points inside R as well as modifying equations (4.25) and (4.27).

4.2. *Calculation of stress intensity factor for rectangular plate with edge crack*

Consider the rectangular plate with edge crack BC = 1 as shown in figure 4*a* where the ends of the plate are subjected to uniformly distributed normal stress $\sigma_n^* = \frac{1}{6}$ with the remainder of the boundary free from traction and constraint. Attention is specifically confined to the calculation of the stress intensity factor, see equations (4.20) and (4.21), at the crack tip located at the point B. Because of symmetry, the problem is readily reduced to one which concerns the square plate ABCDE, shown in figure 4*c*, with side lengths AC = CD = etc. = 3. The kinematic boundary condition u_n^* is then prescribed on C_1 according to

$$u_n^* = 0 \quad \text{on} \quad \text{AB}, \tag{4.29}$$

with traction boundary conditions σ_n^* and/or τ_{ns}^* prescribed on C_2 according to

$$\left.\begin{aligned} \tau_{ns}^* = 0 \quad \text{on ABCDE,} \\ \sigma_n^* = 0 \quad \text{in BCD and EA,} \\ \sigma_n^* = \tfrac{1}{6} \quad \text{on DE.} \end{aligned}\right\} \tag{4.30}$$

The Poisson ratio is taken as $\nu = 0.3$ and the Young modulus E is considered to be unity.

The available computer program accommodates only the first four singular functions $u_k^*(x, y)$ but, notwithstanding the argument which follows equation (4.21), it is still possible to secure a satisfactory piecewise linear solution to the present problem in virtue of the fact that the crack is at the edge of the plate. Because of symmetry about the Ox axis it follows that $\alpha_2 = \alpha_4 = 0$ so that equation (4.21) is further reduced to

$$u^* \simeq u + \alpha_1(u_1^* - u_1) + \alpha_3(u_3^* - u_3). \tag{4.31}$$

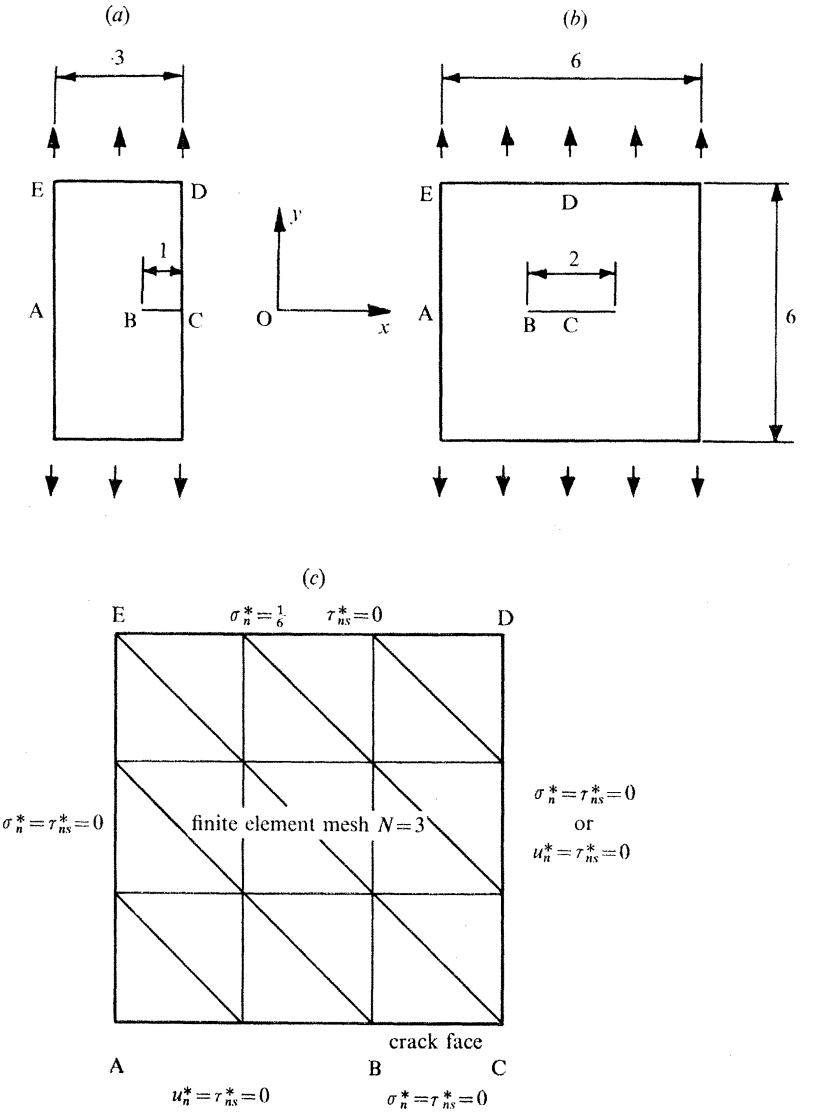

FIGURE 4. Plane stress elasticity problems. (*a*) Rectangular plate with edge crack; (*b*) square plate with central crack; (*c*) reduced problem.

Moreover, in addition to the homogeneous subsidiary condition on C_1 given in equation (4.29) both

$$u_{n1}^* = u_{n3}^* = 0 \quad \text{on} \quad \text{AB}, \tag{4.32}$$

so that equation (4.25) simplifies to

$$D(u_j^* - u_j, u_k^* - u_k) = \int_{C_2} [\sigma_{nk}^*(u_{nj}^* - u_{nj}) + \tau_{nsk}^*(u_{sj}^* - u_{sj})]\, \mathrm{d}s \quad (j, k = 1, 3) \tag{4.33}$$

while, in virtue of equations (4.30), the equation (4.27) simplifies to

$$D(u_j^* - u_j, u^* - u) = \int_{D_E} \tfrac{1}{6}(u_{nj}^* - u_{nj})\,\mathrm{d}s \quad (j = 1, 3). \tag{4.34}$$

Equations (4.16) to (4.20) show that the stress intensity factor (s.i.f.) is given here by

$$\text{s.i.f.} = \alpha_1 - \alpha_3, \tag{4.35}$$

and some values are listed in table 9 for three uniform mesh sizes as controlled by the integer N; the coarsest mesh $N = 3$ is illustrated in figure 4*c*. The calculations are carried out for the two values $a = 1$ and $a = 5$ in this reduced boundary-value problem with open ended crack, and with or without suppressing the term in α_3. For the larger value of a the singular functions $u_j^*(x, y)$ can be combined in such a way as to approximate the well-known corner functions put forward by Williams (1952).

TABLE 9. STRESS INTENSITY FACTORS FOR PLANE STRESS PROBLEM, RECTANGULAR PLATE WITH EDGE CRACK

	semi-length $a = 1$		semi-length $a = 5$	
	one term $\alpha_k = 0, k \neq 1$	two terms $\alpha_k = 0, k \neq 1, 3$	one term $\alpha_k = 0, k \neq 1$	two terms $\alpha_k = 0, k \neq 1, 3$
s.i.f., $N = 3$	0.1786	0.1838	0.1955	0.2008
s.i.f., $N = 6$	0.1955	0.1981	0.2047	0.2061
s.i.f., $N = 12$	0.2035	0.2045	0.2087	0.2087
γ	1.09	1.17	1.21	1.01
c	−0.5028	−0.4439	−0.2911	−0.1491
s.i.f.′	0.2105	0.2095	0.2118	0.2112
s.i.f. long strip (Gross *et al.* (1964))	0.211			

The following abbreviation is used: s.i.f., stress intensity factor $= \alpha_1 - \alpha_3 =$ s.i.f.′$(1 + cN^{-\gamma})$ (say).

In all, twelve values of the s.i.f. are listed in table 9 ranging in magnitude from 0.1786 to 0.2087 and the problem now is to ascertain which is the most accurate value. To avoid the expense of making further advances to successively finer meshes let us attempt an engineering assessment in the light of the experience gathered from the preceding examples. Thus, similarly to equations (2.13) and (3.27) it is assumed over a range of values of N that the s.i.f. behaves like

$$\text{s.i.f.} \simeq \text{s.i.f.}'(1 + cN^{-\gamma}), \tag{4.36}$$

where s.i.f.′ is the extrapolation of s.i.f. for very large values of N and where c and γ have the same meanings as in equation (3.27). Although three different mesh sizes are only just sufficient to determine values for s.i.f.′, c, γ and include the very coarse mesh $N = 3$, the indication from table 9 is that the results in the last column, i.e. for $a = 5$ with retention of the α_3 term, are likely to be the most accurate because $|c|$ is there the smallest. This conclusion is reinforced by a further calculation the results of which are listed in the last row of table 10 where, since it is intended that

$$u_y^*(x, y) \simeq -\alpha v y + \alpha_1 u_{y1}^*(x, y) + \alpha_3 u_{y3}^*(x, y), \tag{4.37}$$

from equation (4.12), should reproduce accurately the analytical structure near the crack tip it follows, on subtraction from equation (4.31), that

$$\alpha v y + u_y(x, y) - \alpha_1 u_{y1}(x, y) - \alpha_3 u_{y3}(x, y) \simeq 0 \tag{4.38}$$

at a point say on the crack face $y = 0^+$ distant 0.25 from the crack tip at B. When $a = 5$, with retention of the α_3 term, table 10 shows that at this point

$$u_y - \alpha_1 u_{y1} - \alpha_3 u_{y3} = -0.0034 \tag{4.39}$$

the magnitude of which should be considered in comparison with $u_y = 0.2948$ at the same point. In the last column of table 9 an extrapolated value s.i.f.$' = 0.2112$, see equation (4.36), is predicted and this bears comparison with the value 0.211 obtained by Cross, Strawley & Brown (1964) using a collocation technique.

TABLE 10. PLANE STRESS PROBLEM OF RECTANGULAR PLATE WITH EDGE CRACK; SOLUTION CHECK ON THE u_y CRACK FACE DISPLACEMENT AT A DISTANCE OF 0.25 FROM THE CRACK TIP AT B, FINITE ELEMENT MESH $N = 12$

	semi-length $a = 1$		semi-length $a = 5$	
	one term $\alpha_k = 0, k \neq 1$	two terms $\alpha_k = 0, k \neq 1, 3$	one term $\alpha_k = 0, k \neq 1$	two terms $\alpha_k = 0, k \neq 1, 3$
u_y	0.2948	0.2948	0.2948	0.2948
$\alpha_1 u_{y1}$	0.2597	0.2740	0.2876	0.4448
$\alpha_2 u_{y2}$	—	−0.0086	—	−0.1466
$u_y - \sum_k \alpha_k u_{yk}$	0.0351	0.0294	0.0072	−0.0034

4.3. *Calculation of stress intensity factor for square plate with central crack*

In this last numerical example the s.i.f. is calculated for a square plate with central crack of length 2BC = 2 as shown in figure 4*b*; the ends of the plate are subjected to a uniformly distributed normal stress $\sigma_n^* = \frac{1}{6}$ with the remainder of the boundary free from traction and constraint. Again, because of symmetry, the problem reduces to one which concerns the square plate ABCDE shown in figure 4*c*, this time with kinematic boundary condition u_n^* prescribed on C_1 according to

$$u_n^* = 0 \quad \text{on} \quad \text{AB and CD}, \tag{4.40}$$

and tractions σ_n^* and/or τ_{ns}^* prescribed on C_2 according to

$$\left.\begin{aligned} \tau_{ns}^* &= 0 \quad \text{on} \quad \text{ABCDE}, \\ \sigma_n^* &= 0 \quad \text{on} \quad \text{BC and EA}, \\ \sigma_n^* &= \tfrac{1}{6} \quad \text{on} \quad \text{DE}. \end{aligned}\right\} \tag{4.41}$$

Details of the modified Rayleigh–Ritz solution follow closely those already described in § 4.2 except that it is no longer possible to simplify the equation (4.25). Twelve values of the s.i.f. are listed in table 11 where there is seen to be quite substantial variation in magnitude ranging from 0.1122 to 0.1916. Analysis of the results by fitting equation (4.36) shows this time, however, that the results in the first column, i.e. for $a = 1$ with the term in α_3 suppressed, are likely to be the most accurate because of the appreciably smaller value which is attained by $|c|$. This conclusion is confirmed after examining the accuracy of the analytical representation of the u_y displacement on the crack face (cf. equations (4.37) to (4.39)), the results of which are listed in table 12. The extrapolated value s.i.f.$' = 0.1365$ in the first column of table 11 is somewhat larger (as is to be expected), than the s.i.f. = 0.1255 provided by Koiter's (1965) formula (Rooke 1970) appropriate to an infinitely long strip.

The values of the s.i.f. which are obtained for crack semi-length $a = 1$ are especially interesting.

When the term in α_3 is retained then table 11 shows that the s.i.f. converges like $N^{-1.94}$ which is very near the best available rate, but this solution is not satisfactory because of the large value of c (0.4468). The evidence shows that a better result is actually obtained by suppressing the term in α_3 which should really be suppressed also in virtue of symmetry. This experiment highlights the need for prudence in selecting suitable forms for the singular functions as well as demonstrating that the inclusion of additional terms does not necessarily lead to an improved result for the s.i.f.

TABLE 11. STRESS INTENSITY FACTORS FOR PLANE STRESS PROBLEM, SQUARE PLATE WITH CENTRAL CRACK

	semi-length $a = 1$		semi-length $a = 5$	
	one term $\alpha_k = 0, k \neq 1$	two terms $\alpha_k = 0, k \neq 1, 3$	one term $\alpha_k = 0, k \neq 1$	two terms $\alpha_k = 0, k \neq 1, 3$
s.i.f., $N = 3$	0.1313	0.1916	0.1124	0.1122
s.i.f., $N = 6$	0.1335	0.1525	0.1237	0.1237
s.i.f., $N = 12$	0.1348	0.1423	0.1303	0.1303
γ	0.81	1.94	0.79	0.79
c	−0.0923	0.4468	−0.4600	−0.4656
s.i.f.′	0.1365	0.1387	0.1393	0.1393
s.i.f. infinite strip (Rooke (1970))	0.1255			

The following abbreviation is used: s.i.f., stress intensity factor $= \alpha_1 - \alpha_3 =$ s.i.f.′$(1 + cN^{-\gamma})$ (say).

TABLE 12. PLANE STRESS PROBLEM OF SQUARE PLATE WITH CENTRAL CRACK; SOLUTION CHECK ON THE u_y CRACK FACE DISPLACEMENT AT A DISTANCE OF 0.25 FROM THE CRACK TIP AT B, FINITE ELEMENT MESH $N = 12$

	semi-length $a = 1$		semi-length $a = 5$	
	one term $\alpha_k = 0, k \neq 1$	two terms $\alpha_k = 0, k \neq 1, 3$	one term $\alpha_k = 0, k \neq 1$	two terms $\alpha_k = 0, k \neq 1, 3$
u_y	0.1903	0.1903	0.1903	0.1903
$\alpha_1 u_{y1}$	0.1881	0.2250	0.1965	0.1792
$\alpha_2 u_{y2}$	—	−0.0176	—	0.0161
$u_y - \sum_k \alpha_k u_{yk}$	0.0021	−0.0172	−0.0062	−0.0050

5. CONCLUSIONS

A practical and very general method of calculation has been described and demonstrated for the finite element solution of boundary value problems with non-removable singularities. Particular attention is given to the assessment of the achieved accuracy and the rate of convergence of the numerical solutions.

The method broadly resolves into four stages as follows.

(i) A solution of the base problem using the piecewise polynomial coordinate functions in the ordinary Rayleigh–Ritz method.

(ii) The purely analytical structure of each singularity is then described in terms of appropriate functions.

(iii) Substitution of these functions into the homogeneous form of the governing field equation provides individual boundary-value problems each of which are solved by the ordinary Rayleigh–Ritz method using *identical* coordinate functions to those of stage (i).

(iv) The difference between the functions of stage (ii) and the Rayleigh-Ritz solution of stage (iii) are then used to augment the ordinary coordinate functions of the stage (i) solution to the base problem. Because of underlying orthogonality relations it is permissible to determine the amplitudes of these augmenting coordinate functions by a separate Rayleigh–Ritz calculation which provides a set of linear simultaneous equations equal in number to that of the singularities.

Thus, it is formally acceptable to describe the analytical structure of the singularities by simple functions which satisfy the governing field equation only at the singular points. Although experience from the worked examples shows that it is preferable to avoid the use of special regions around the singularities, there may be compelling and overriding reasons to introduce such regions in certain circumstances. Then, an idea may be pursued from Fix (1969) where the special regions are so faired that the requisite piecewise continuity is maintained throughout the whole enclosed region.

The presence of singularities is of special significance in fracture mechanics where there is scope for extensive numerical experimentation by engineers questing for rapid, yet reliable, estimates of the related stress intensity factors. Some specific matters concern.

(1) The most effective and convenient means of representing the analytical structure of singularities. In complex structures there are likely to be compelling reasons to employ special regions. Assessment is required of relative sizing of such regions and whether it is then practically worthwhile to maintain continuity of the early derivatives of the singular functions. Indeed, under certain circumstances it may not be practically worthwhile to maintain exact continuity of the singular function itself, cf. the super element approach.

(2) In some problems it is difficult enough to find augmenting singular functions which satisfy the governing homogeneous partial differential equation just at the singular point. Indeed, the partial differential equation itself may be known only in the immediate locality. Experience is required of these situations; it may be advisable to refine the mesh size near such singular points.

(3) It is not known whether there is computational advantage in employing higher degree polynomial representation for the ordinary finite element scheme when the sole objective is to determine the amplitude of the singularity.

References

Byskov, E. 1970 *Int. J. Fracture Mech.* **6**, 159.
Fix, G. 1969 *J. math. Mech.* **18**, 645.
Fox, L. 1971 *Proc. R. Soc. Lond.* A **323**, 179.
Gross, B., Srawley, J. E. & Brown, W. F. 1964 *NASA Tech. Note* D-2395.
Koiter, W. T. 1965 *Tech. Univ. Delft, Dep. Mech. Eng. Rep.* no. 314.
Morley, L. S. D. 1963 *Skew plates and swept structures*. Pergamon Press.
Morley, L. S. D. 1969 *J. mech. phys. Solids* **17**, 73.
Morley, L. S. D. 1970 *Int. J. num. Methods Engng* **2**, 85.
Motz, H. 1946 *Q. appl. Math.* **4**, 371.
Muskhelishvilli, N. I. 1953 *Some basic problems of the mathematical theory of elasticity*. Groningen: Noordhoff.
Newman, J. C. 1971 *NASA Tech. Note* D-6376.
Pian, T. H. H., Tong, P. & Luk, C. H. 1971 Elastic crack analysis by a finite element hybrid method. In *Air Force 3rd Conference on Matrix Methods in Structural Mechanics*. Wright Patterson Air Force Base, Ohio, U.S.A.
Rooke, D. P. 1970 *Engng Fract. Mech.* **1**, 727.
Sneddon, I. N. & Lowengrub, M. 1969 *Crack problems in the classical theory of elasticity*. New York: Wiley.
Walsh, Joan 1971 *Proc. R. Soc. Lond.* A **323**, 155.
Whiteman, J. R. 1971 *Proc. R. Soc. Lond.* A **323**, 271.
Williams, M. L. 1952 *J. appl. Mech.* **19**, 526.
Wilson, W. K. 1969 *On combined mode fracture mechanics*. Ph.D. Thesis, University of Pittsburgh.
Woods, L. 1953 *Q. Jl mech. appl. Math.* **6**, 163.
Zlamal, M. 1968 *Numer. Math.* **12**, 394.

PHILOSOPHICAL TRANSACTIONS OF THE ROYAL SOCIETY A MATHEMATICAL, PHYSICAL & ENGINEERING SCIENCES